Korean J. Chem. Eng., **29**(10), 1285-1288 (2012)
DOI: 10.1007/s11814-012-0074-4

RAPID COMMUNICATION

One-step synthesis of mesoporous sulfated zirconia nanoparticles with anionic template

Hongping Pu, Liuyi Zhang, Dongquan Du, Caiyun Han, Hongyin Li, Jiangyan Li, and Yongming Luo†

Faculty of Environmental Science and Engineering, Kunming University of Science and Technology, Kunming 650093, P. R. China

(*Received 1 February 2012 • accepted 22 May 2012*)

Abstract–Mesoporous sulfated zirconia nanoparticles (MSZNP) with high surface area have been synthesized by using sodium dodecyl sulfate ($C_{12}H_{25}OSO_3Na$, SDS), both as a template and a sulfating agent via one-step route. On the basis of FT-IR, EDS together with NH_3-TPD analyses, the SO_4^{2-} anion, originated from the hydrophilic head of SDS, can be incorporated into ZrO_2 to form MSZNP with super-acidity. The phase transition of ZrO_2 from tetragonal to monoclinic phase was effectively inhibited by the presence of SO_4^{2-}, and the formation mechanism was illustrated in detail. $MSZNP_{(550)}$ achieved far higher activity than $CSZ_{(550)}$ in transesterification of soybean oil with methanol due to the synergistic effect of strong acidity, high BET surface area and the formation of mesostructure.

Key words: Sulfated Zirconia, Nanoparticles, Porous Materials, One-step Route, Transesterification

INTRODUCTION

Sulfated zirconia has been intensively applied for numerous important industrial and organic reactions [1-3]. It is well documented that mesoporous sulfated zirconia (MSZ) exhibits much higher catalytic activity than conventional sulfated zirconia (CSZ) owing to the synergic effect of high surface area, uniform pore size and large porosity [4-7]. Therefore, many researchers have focused on the synthesis of MSZ with high surface area [8-19], and these synthesis routes can be generally classified into one-step and two-step. Compared with two-step, one-step synthesis route has attracted much attention due to the advantages of avoiding sulfating step and simplifying the overall synthesis procedure to a great extent [1,17]. Schüth et al. reported MSZ was synthesized by employing CTAB as a structure-directing agent via one-step LCT method for the first time [19]. SDS as a template was first used to synthesize mesoporous zirconia rather than MSZ [20]. Recently, Ozawa et al. attempted to synthesize MSZ with $Zr(OC_3H_7)_4$ and SDS via an one-step route. However, mesostructure, confirmed by their small angle XRD, was not formed at all, and BET surface area of the calcined sample (600 °C for 1 h) is only 24 m^2/g [21].

In this contribution, we report a new one-step route for the synthesis of MSZ nanoparticles with high surface area by using SDS both as a template and a sulfating agent. The formation mechanism and catalytic activity are investigated. Catalytic data show that $MSZNP_{(550)}$ exhibits higher activity than $CSZ_{(550)}$ in transesterification of soybean oil with methanol.

EXPERIMENTAL

1. Synthesis of Catalyst

The following general procedure was used to prepare mesoporous sulfated zirconia nanoparticles (MSZNP) described in this article. $Zr(OC_3H_7)_4$ and SDS were used as a zirconium source and a structure-directing agent, respectively. In a typical synthesis batch, 13.5 g of SDS was added into 200 ml of deionized water with vigorous stirring at room temperature (RT). After SDS was dissolved completely, calculated $Zr(OC_3H_7)_4$ was added into the mixture solution to keep the molar ratio of Zr/S between 0.25 and 4.0. Next, the pH value of mixture solution was adjusted by using HCl (1.0 M) to 3.0 and the mixture solution was stirred for 0.5 h. Then, the mixture was aged at RT for 20 h and thermally treated at 80 °C for five days under static conditions in turn. Subsequently, the reaction product was filtered, washed with the mixture solution of deionized water and isopropanol and dried at 110 °C for 12-24 h. Finally, the sample was calcined at various temperatures (400 °C, 550 °C, 650 °C and 750 °C) in air for 3 h. As-synthesized and calcined samples were termed as $MSZNP_{(AS)}$ and $MSZNP_{(x)}$, where "x" is calcination temperature.

For comparison purposes, conventional sulfated zirconia (CSZ) was synthesized by using the traditional two-step method. In a typical synthesis batch, 20 ml of $Zr(OC_3H_7)_4$ was added into 200 ml of H_2O. Next, the pH value of mixture solution was adjusted by using 1.0 M HCl to 3.0 and the mixture solution was continuously stirred for 0.5 h. The mixture was aged at RT for 20 h and thermally treated at 80 °C for five days under static conditions in sequence. After that, the white reaction product $Zr(OH)_4$ was filtered, washed with the mixture solution of deionized water and isopropanol and dried at 110 °C for 12-24 h. The dried zirconium hydroxide was ground and was added into 1.0 M H_2SO_4 solution with stirring (20 ml/g $Zr(OH)_4$) for 2 h. Then, the sulfated product was filtered and dried again at 110 °C for 12-24 h. Finally, the sample was calcined at 550 °C in air for 3 h. The sulfated zirconia sample synthesized by this route was designated as $CSZ_{(550)}$.

2. Characterization

X-ray diffraction (XRD) patterns were performed on a Rigaku D/max-1200 diffractometer using Cu K_α radiation (λ=1.5406 Å), operating at 40 kV and 30 mA. BET surface area and N_2 adsorption-desorption isotherms were carried out on a Micromeritics-ASAP-

†To whom correspondence should be addressed.
E-mail: luoyongming@tsinghua.org.cn

2000 apparatus at −196 °C. All samples were degassed at 250 °C for 2 h prior to analysis. The BET specific surface area was calculated from adsorption data in the relative pressure range from 0.05 to 0.25. TEM and HR-TEM images were obtained on a JEM-2010 HR transmission electron microscope, operating with an acceleration voltage of 200 kV. FT-IR spectra of the samples in the form of KBr pellets were recorded by using a Nicolet 560 IR spectrometer. The NH_3 temperature programmed desorption (NH_3-TPD) measurements were carried on an Autochem 2910 instrument, and a thermal conductivity detector was used for continuous monitoring of desorbed ammonia. Prior to TPD analysis, the sample was pretreated at 400 °C for 1 h in a flow of ultra pure helium gas (40 ml/min), and the sample was cooled to 100 °C in the flow of ultra pure helium gas. The pretreated sample was then saturated with 10% anhydrous ammonia gas (balance He, 60 ml/min) at 50 °C for 2 h and subsequently flushed with He (60 ml/min) at 100 °C for 2 h to remove the physisorbed ammonia. The heating rate of the TPD measurements, ranging from 100 °C to 700 °C, was 10 °C/min.

3. Transesterification of Soybean Oil with Methanol

Transesterification experiments of soybean oil with methanol over $MSZNP_{(550)}$ and $CSZ_{(550)}$ were performed in a stirred batch reactor with samples withdrawn periodically for analysis, and the detailed reaction conditions were as follows: 1) reaction temperature was kept at 120 °C; 2) the mole ratio of methanol to soybean oil was maintained 12; and 3) the amount of catalysts ($MSZNP_{(550)}$ or $CSZ_{(550)}$) is 4 wt% of soybean oil. The yield of fatty acid methyl esters (FAME) was determined by a flame ionization detection-gas chromatograph equipped with a capillary column (Agilent DB-5HT, 30 m×0.32 mm ×0.10 μm).

RESULTS AND DISCUSSION

Fig. 1 provides an N_2 adsorption-desorption isotherm and BJH pore size distribution curve of $MSZNP_{(AS)}$. According to IUPAC classification, the N_2 adsorption-desorption isotherm of $MSZNP_{(AS)}$ is found to be of type IV. Three well distinguished regions (monolayer-multilayer adsorption; capillary condensation as well as multilayer adsorption on the outer particle surface) of the adsorption isotherm are evident, and a narrow BJH pore size distribution with average diameter of 2.9 nm is observed. The presence of a single diffraction peak in 2θ region below 2° for the sample (Fig. S1 in Supplementary Materials) is indicative of a disordered mesostructure [22-24]. Compared with $MSZNP_{(AS)}$, similar N_2 sorption isotherms are observed for the sample after calcination ($MSZNP_{(550)}$), thus further indicating the presence of mesostructure within $MSZNP_{(550)}$ (see Fig. S2 in Supplementary Materials). BET surface areas of $MSZNP_{(AS)}$, $MSZNP_{(400)}$, $MSZNP_{(550)}$, $MSZNP_{(650)}$ and $CSZ_{(550)}$ are summarized in Table S1 (see Supplementary Materials). Obviously, the BET surface area of $MSZNP_{(550)}$ is 162 m^2/g, which is far higher than $CSZ_{(550)}$ as well as the sulfated zirconia samples prepared with other conventional two-step method [13,19].

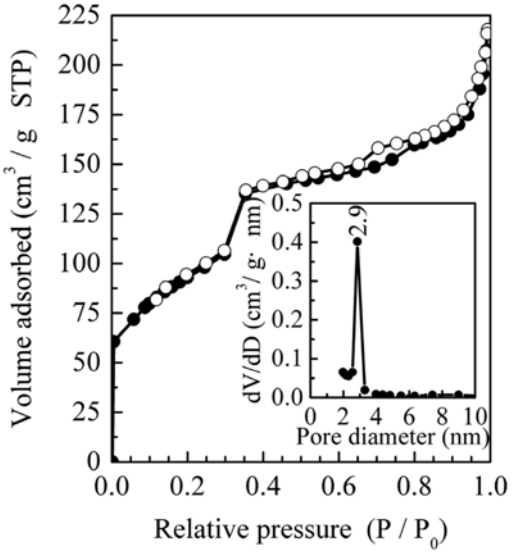

Fig. 1. N_2 adsorption-desorption isotherm and BJH pore size distribution of $MSZNP_{(AS)}$.

FT-IR spectra of $MSZNP_{(AS)}$ and $MSZNP_{(550)}$ are displayed in Fig. 2. The bands centered at 1,058, 1,130 and 1,219 cm^{-1}, ascribed to characteristic vibrations of chelating bidentate sulphate anion [18, 25], are well-expressed in the spectra of $MSZNP_{(AS)}$ and $MSZNP_{(550)}$. However, the band intensities of $MSZNP_{(550)}$ are weaker than those of $MSZNP_{(AS)}$ due to the loss of sulfuric species in the course of high temperature calcination. Three bands centered at 1,464, 2,849 and 2,925 cm^{-1} are observed in the spectrum of $MSZNP_{(AS)}$, but not for $MSZNP_{(550)}$, which have been attributed to the asymmetric stretching vibration of methyl groups (CH_3), and asymmetric as well as symmetric stretching modes of methylene groups (CH_2) [26,27]. On the basis of FT-IR analyses, it can be concluded that SO_4^{2-} anion was incorporated into $MSZNP_{(550)}$ and the template of SDS was completely removed.

It was well documented that the tetragonal ZrO_2 is more active in catalysis [9,28-30]. XRD patterns of $MSZNP_{(AS)}$, $MSZNP_{(550)}$, $MSZNP_{(550)}$ and $MSZNP_{(650)}$ are presented in Fig. 3. Five diffraction peaks, indexed to (111), (200), (220), (311) and (222) reflections of tetragonal ZrO_2, are observed for $MSZNP_{(550)}$, corresponding to a primary crystal size of ca. 7.0 nm calculated by using the Scherrer equation. Generally, the phase transformation of pure ZrO_2 from tetragonal to monoclinic occurs at temperature range of 500-600 °C [8,31]. However, $MSZNP_{(550)}$ only contains tetragonal ZrO_2, and only a very

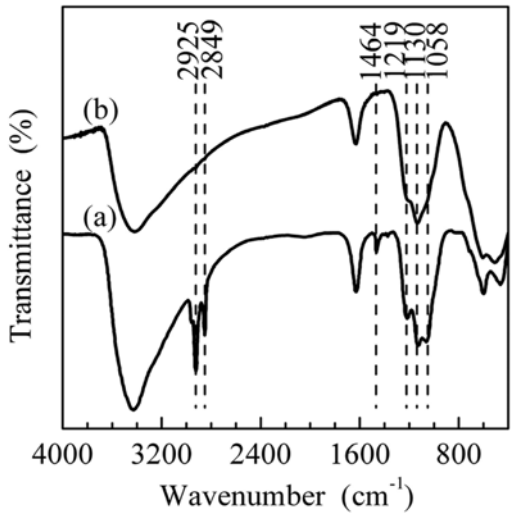

Fig. 2. FT-IR spectra of (a) $MSZNP_{(AS)}$ and (b) $MSZNP_{(550)}$.

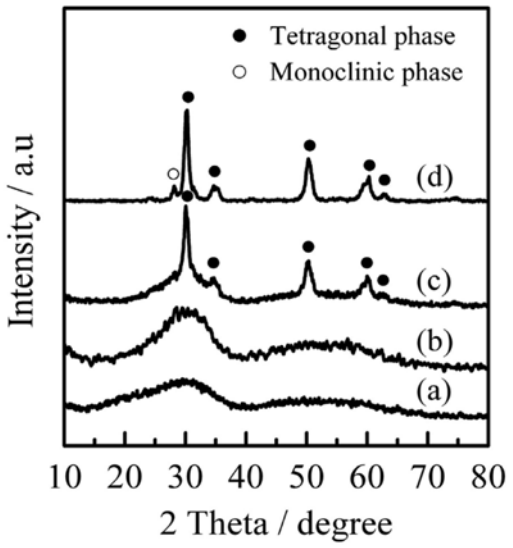

Fig. 3. XRD patterns of (a) $MSZNP_{(AS)}$, (b) $MSZNP_{(400)}$, (c) $MSZNP_{(550)}$ and $MSZNP_{(650)}$.

weak monoclinic ZrO_2 diffraction peak is detected for $MSZNP_{(650)}$. These results suggest that tetragonal ZrO_2 within $MSZNP_{(AS)}$ is more stable than pure ZrO_2. This expected phase transition from tetragonal to monoclinic ZrO_2 is most likely inhibited by the SO_4^{2-} covered on the surface that can effectively prevent the conglomeration between ZrO_2 clusters.

From bright-dark TEM image, small particles with average diameter of 7.2 nm can be identified (Fig. 4(A)). Three elements (Zr, O and S) are distinctly observed in the EDS profile of $MSZNP_{(550)}$, thus indicating these nanoparticles are sulfated zirconia rather than zirconia (inset in Fig. 4(A)). Further quantitative analysis shows that the S content of $MSZNP_{(550)}$ is 3.74 wt%, which is comparable to $CSZ_{(550)}$ (3.66 wt%). The orientation of nanoparticles with well-defined lattice planes is observed for $MSZNP_{(550)}$ (Fig. 4(B)), and the spacing distance inferred from the lattice planes is ascribable to the (111) crystal planes of tetragonal ZrO_2, which is well consistent with XRD results that $MSZNP_{(550)}$ only contains tetragonal ZrO_2 and the primary crystal size is 7.0 nm.

Two NH_3 desorption peaks are detected for both $MSZNP_{(550)}$ and $CSZ_{(550)}$, while the desorption temperature of $MSZNP_{(550)}$ slightly shifts to high-temperature region compared with $CSZ_{(550)}$, indicating the acidity of $MSZNP_{(550)}$ is stronger than $CSZ_{(550)}$ (see Fig. S2 in Supplementary Materials).

The formation mechanism is illustrated in Fig. S4 (in Supplementary Materials). SDS was dissolved in water to yield $C_{12}H_{25}OSO_3^-$ anion, which contains one hydrophobic and one hydrophilic head. It was demonstrated that the isoelectric point of ZrO_2 is about 5.6 [32,33]. Therefore, when the pH was adjusted to 3.0 by dropwise adding HCl into synthesis media, positive zirconium species were formed via hydrolysis of $Zr(OC_3H_7)_4$. Then, the positive zirconium species interacted with the hydrophilic head of $C_{12}H_{25}OSO_3^-$ via electrostatic interaction to form inorganic and organic hybrids (Fig. S4(a)). The composites containing template and zirconium species (Fig. S4(d)) were obtained via two possible pathways. In the first pathway (steps a and a′), the self-assembly step (a′) to form circular structure occurs only after sufficient propagation of the polycondensation hybrids (Fig. S4(b)). In the second pathway (steps b and b′), the micellar arrays structure (Fig. S4(c)) was formed prior to subsequent condensation (b′). Finally, the template SDS was removed when the resulting product was calcined, as evidenced by FT-IR. At the same time, the SO_4^{2-} anion, originating from the hydrophilic moieties of SDS, was incorporated into zirconia due to the direct strong interaction between the zirconium species and sulfated species.

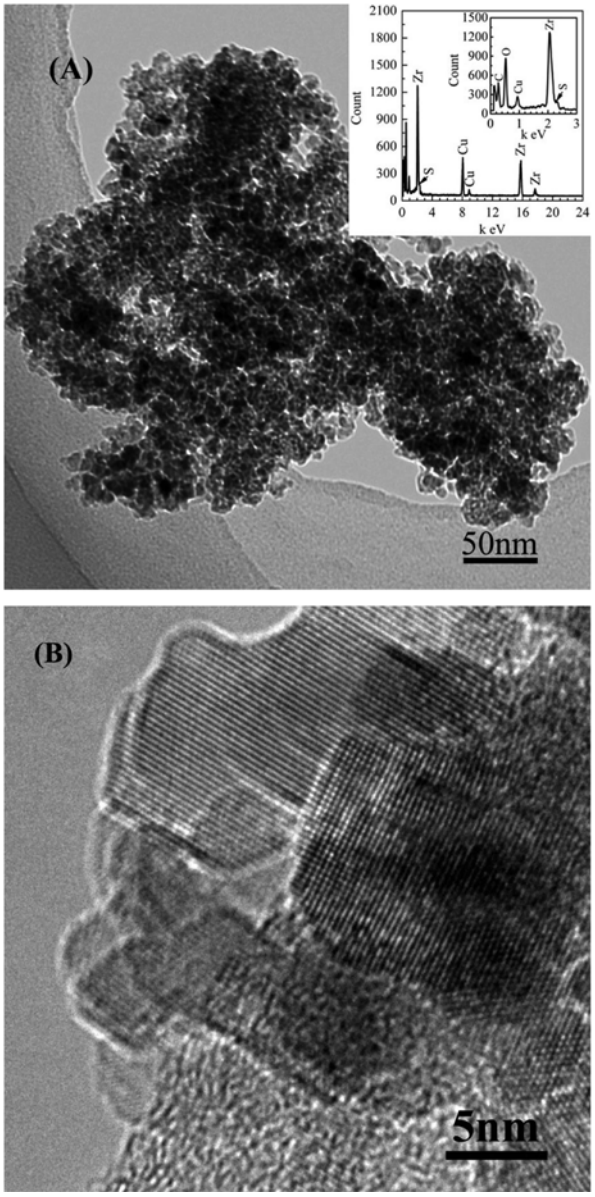

Fig. 4. (A) TEM image and EDS profile (inset) and (B) HR-TEM images of $MSZNP_{(550)}$.

Fig. 5 illustrates the transesterification of soybean oil with methanol over $MSZNP_{(550)}$ and $CSZ_{(550)}$. It is clear that the fatty acid methyl ester (FAME) yield of $MSZNP_{(550)}$ in transesterification of soybean oil with methanol is higher than $CSZ_{(550)}$. The difference between $MSZNP_{(550)}$ and $CSZ_{(550)}$ can be explained as follows: the acidity of the former is stronger than that of $CSZ_{(550)}$, as evidenced by NH_3-TPD. On the other hand, mesostructure together with high BET surface area of $MSZNP_{(550)}$ is less susceptible to pore blockage, which will be favorable for the transport of reactants and products [34-37].

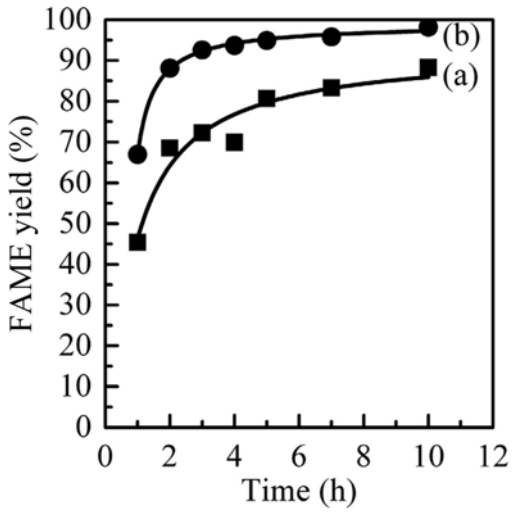

Fig. 5. Transesterification of soybean oil with methanol over (a) $CSZ_{(550)}$ and (b) $MSZNP_{(550)}$. Reaction conditions: temperature 120 °C; amount of catalyst 4% (w/w, soybean oil); mole ratio (methanol to soybean oil)=12.

In summary, we report a new one-step route for synthesis of mesoporous sulfated zirconia nanoparticles (MSZNP) by using SDS both as a template and a sulfating agent. It was demonstrated that the SO_4^{2-} anion, which originated from the hydrophilic moieties of SDS, can be easily incorporated into zirconia to form superacid, and the formation mechanism is illustrated. $MSZNP_{(550)}$ exhibits higher activity than $CSZ_{(550)}$ in transesterification of soybean oil with methanol owing to the synergistic effect of strong acidity, high BET surface area and the formation of mesostructure.

ACKNOWLEDGMENTS

We gratefully acknowledge the support of this research work by the National Natural Science Foundation of China (Grant No. 20867003, 21003066 and 51068010), China Postdoctoral Science Foundation Funded Project (Grant No. 20100471686), Young Academic and Technical Leader Raising Foundation of Yunnan Province (Grant No. 2008py010).

SUPPORTING INFORMATION

Additional information as noted in the text. This information is available via the Internet at http://www.springer.com/chemistry/journal/11814.

REFERENCES

1. B. M. Reddy and M. K. Patil, *Chem. Rev.*, **109**, 2185 (2009).
2. L. Y. Zhang, C. Y. Han, D. Q. Du, Y. Y. Zhang, S. W. Xu and Y. M. Luo, *Prog. Chem.*, **23**, 860 (2011).
3. X. M. Song and A. Sayari, *Catal. Rev. Sci. Eng.*, **38**, 329 (1996).
4. E. Zhao, S. E. Hardcastle, G. Pacheco, A. Garcia, A. L. Blumenfeld and J. J. Fripiat, *Micropor. Mesopor. Mater.*, **31**, 9 (1999).
5. X. Yang, F. C. Jentoft, R. E. Jentoft, F. Girgsdies and T. Ressler, *Catal. Lett.*, **81**, 25 (2002).
6. M. A. Risch and E. E. Wolf, *Appl. Catal. A: Gen.*, **172**, L1 (1998).
7. M. Risch and E. E. Wolf, *Catal. Today*, **62**, 255 (2000).
8. M. K. Mishra, B. Tyagi and R. V. Jasra, *Ind. Eng. Chem. Res.*, **42**, 5727 (2003).
9. M. Risch and E. E. Wolf, *Appl. Catal. A. Gen.*, **206**, 283 (2001).
10. Y. W. Suh, J. W. Lee and H. K. Rhee, *Appl. Catal. A. Gen.*, **274**, 159 (2004).
11. V. G. Devulapelli and H. S. Weng, *Catal. Commun.*, **10**, 1711 (2009).
12. M. Lutecki, O. Solcova, S. Werner and C. Breitkopf, *J. Sol.-Gel. Sci. Technol.*, **53**, 13 (2010).
13. D. J. McIntosh and R. A. Kydd, *Micropor. Mesopor. Mater.*, **37**, 281 (2000).
14. M. Signoretto, A. Breda, F. Somma, F. Pinna and G. Cruciani, *Micropor. Mesopor. Mater.*, **91**, 23 (2006).
15. Y. Y. Sun, L. Yuan, W. Wang, C. L. Chen and F. S. Xiao, *Catal. Lett.*, **87**, 57 (2003).
16. S. K. Das, M. K. Bhunia, A. K. Sinha and A. Bhaumik, *J. Phys. Chem. C*, **113**, 8918 (2009).
17. S. Melada, S. A. Ardizzone and C. L. Bianchi, *Micropor. Mesopor. Mater.*, **73**, 203 (2004).
18. Y. Y. Sun, S. Q. Ma, Y. C. Du, L. Yuan, S. C. Wang, J. Yang, F. Deng and F. S. Xiao, *J. Phys. Chem. B*, **109**, 2567 (2005).
19. U. Ciesla, S. Schacht, G. D. Stucky and F. Schüth, *Angew. Chem. Int. Ed.*, **35**, 541 (1996).
20. G. Pacheco, E. Zhao, A. Garcia, A. Sklyarov and J. J. Fripiat, *Chem. Commun.*, 491 (1997).
21. M. Ozawa, D. Yokoi and S. Suzuki, *J. Mater. Sci. Lett.*, **22**, 1543 (2003).
22. P. T. Tanev and T. J. Pinnavaia, *Science*, **267**, 865 (1995).
23. S. Cabrera, J. E. Haskouri, J. Alamo, A. Beltrán, D. Beltrán, S. Mendioroz, M. D. Marcos and P. Amorós, *Adv. Mater.*, **11**, 379 (1999).
24. Y. M. Luo, Z. Y. Hou, D. F. Jin, J. Gao and X. M. Zheng, *Mater. Lett.*, **60**, 393 (2006).
25. F. Babou, G. Coudurier and J. C. Vedrine, *J. Catal.*, **152**, 341 (1995).
26. V. Lochaø, *Appl. Catal. A. Gen.*, **309**, 33 (2006).
27. H. G. Bernal, L. C. Caero, E. Finocchio and G. Busca, *Appl. Catal. A. Gen.*, **369**, 27 (2009).
28. G. Pacheco, E. Zhao, E. D. Valdes, A. Garcia and J. J. Fripiat, *Micropor. Mesopor. Mater.*, **32**, 175 (1999).
29. T. Yamaguchi, *Catal. Today*, **20**, 199 (1994).
30. B. M. Reddy, P. M. Sreekanth and V. R.Reddy, *J. Mol. Catal. A. Chem.*, **225**, 71 (2005).
31. A. D'Epifanio, M. A. Navarra, F. C. Weise, B. Mecheri, J. Farrington, S. Licoccia and S. Greenbaum, *Chem. Mater.*, **22**, 813 (2010).
32. K. D. Hristovski, P. K. Westerhoff, J. C. Crittenden and L. W. Olson, *Environ. Sci. Technol.*, **42**, 3786 (2008).
33. K. Hristovski, A. Baumgardner and P. Westerhoff, *J. Hazard. Mater.*, **147**, 265 (2007).
34. H. Wang, C. Y. Han, H. P. Pu, L. Y. Zhang, Z. H. Zou and Y. M. Luo, *Bull. Chem. Soc. Jpn.*, **83**, 852 (2010).
35. Y. M. Luo, Z. Y. Hou, R. T. Li and X. M. Zheng, *Can. J. Chem.*, **85**, 379 (2007).
36. M. A. Harmer, W. E. Farneth and Q. Sun, *Adv. Mater.*, **10**, 1255 (1998).
37. W. M. van Rhijn, D. E. de Vos, B. F. Sels, W. D. Bossaert and P. A. Jacobs, *Chem. Commun.*, 317 (1998).